Journal of GEOLOGY, series B, No, 53-54/2021, p38-61

Microfacies and diagenesis of the lower part of Upper Cambrian carbonate succession in the Lung Cu outcrop, Dong Van area in Northeast Vietnam

Nguyen Duc Phong

Vietnam Institute of Geosciences and Mineral Resources (VIGMR),

67 Chien Thang, Van Quan, Ha Dong, Ha Noi, Vietnam

E-mail: phongcs@gmail.com

Received date:15/08/2021

Accepted date:30/12/2021

Key words: *Microfacies, Diagenesis, Cambrian, Lung Cu, Dong Van, Hà Giang, Vietnam*

Abstract*: In the Dong Van area in northeast Vietnam, lower part of Upper Cambrian carbonate succession, more specifically the lower part of Chang Pung Formation in the Lung Cu outcrop consists of a succession of oolitic pack- to grainstones, oncolite pack- to grainstones, intraclast to lithoclast grainstones, wackestone and mudstones. The integration of microfacies and diagenesis of these carbonate successions in the Lung Cu outcrop are interpreted based on conventional microscopy and cathodoluminescence (CL) microscopy analysis. On the basis of lithology, texture, grain composition, and sedimentary structures, eight microfacies have been recognized including:1- Marl (Facies 1); 2- Parallel bedded limestone (Facies 2); 3- Wavy bedded limestone (Facies 3); 4- Oncoid- intraclast (Facies 4); 5- Floatstone-intraclast-extraclast (Facies 5); 6- Bioclast-lithoclast-ooid (Facies 6); 7- Ooid-bioclast-oncoid (Facies 7); 8- Ooid-lithoclast (Facies 8). These microfacies reflect deposition in peritidal to mid-ramp in shallow-marine depositional environments with differences in wavy energy conditions in the near tropical conditions of the South China plate. Diagenetic processes identified consist of micritization, cementation, dissolution, dolomitization and dedolomitization and compaction. These processes reflect syndepositional marine, subaerial meteoric, near-surface marine, vadose-marine and meteoric-phreatic diagenetic realms. Of importance is the presence of paleokarsts originated where shallow marine limestones have become subaerially exposed by a fall in relative sea level.*

1. Introduction

The Middle Cambrian - Lower Ordovician carbonate - siliciclastic rocks containing trilobites, brachiopods and crinoids in the Dong Van area in northeast Vietnam were investigated and studied at varying degrees on paleontology and stratigraphy. The differences in the stratigraphic division are variable in thickness, age, stratigraphic relationships as well as in terms of lithostratigraphic contents. The dating and stratigraphic correlation of sedimentary rocks are mainly based on paleontological materials. Previous studies in this area have focused on stratigraphic and biostratigraphical characteristics (Depart., 1915, 1916; Mansuy., 1915, 1916, Kobayashi., 1944; Saurin., 1956; Dovjikov et al., 1965; Tinh., 1976, 2001), and have not yet addressed the microfacies and diagenesis of these rocks. The integration of microfacies and diagenesis has great potential for refining questions relating to paleoenvironmental

changes and diagenetic history of a carbonate platform and its control on (paleo)karst development. In this respect carbonate grains such as ooids, peloids, oncolites, cortoids, pisoids, fossils or pre-existing carbonate fragments are valuable proxies for high-resolution palaeoenvironmental studies. From a diagenetic point of view, (paleo)karstification can be considered as one of the different but important processes affecting carbonate sediments (Wright and Smart, 1994). Early diagenetic dolomitization and karstification are common features in shallow-water carbonates and have been reported throughout the geologic record (Goldhammer et al., 1990; Montañez and Read, 1992; Wright and Smart, 1994; Yoo and Lee, 1998; Bosence et al., 2000; Dehler et al., 2001). Their patterns, processes, and timing frequently play a key role in understanding the development of carbonate platforms. This study provides new data on the microfacies and the diagenetic characteristics for the lower part of Upper Cambrian carbonate succession in the Lung Cu outcrop, in order to reconstruct a depositional model and diagenetic paragenetic sequences; consequently, detailed information on the petrography of these carbonates, including conventional microscopy and cathodoluminescence (CL) microscopy will be reported.

2. Geological setting

The Lung Cu outcrop ($23^0$21'97"N; $105^0$18'89"E) at Lung Cu village, 25 km north of Dong Van District Town, is a type section for the Late Cambrian carbonates. This outcrop is located adjacent to the Vietnamese - Chinese border at the northernmost place of Vietnam and is magnificently exposed as a huge hogback succession seen from the Lung Cu Flag visitor center (*Figure 4*, Photo 1). In this outcrop the carbonate succession of the Chang Pung Formation is well exposed. These strata are mainly composed of regularly dipping beds of carbonate sediments - micrite limestone, dolomitic limestone, oolitic limestone interbedded with argillaceous shale, siltstone and sandstone; containing shallow-water marine fauna with trilobites and brachiopods. The age of Chang Pung Formation is not unequivocal, i.e. a Late Cambrian age has been proposed by most authors.

In the Late Cambrian, the South China plate was part of Asian blocks originated as spli-off terranes of Gondwana, including the southern part of China and northeastern fragment of Vietnam. This area was separated from North China by the Quingling-Dabie suture, from Indochina by the Song Ma suture, from the Sibumasu terrane by the Ailaoshan suture and from the Songpan-Ganzi accretionary complex by the Longmenshan suture (*Figure 3*) (Nie *et al*., 1990; Metcalfe, 1998, 2005). Paleolatitudinal position was between 1^0 and 15^0 for the South China area in the Late Cambrian. Faunas of this age on the Asian blocks and in Australasia allow defining an Asian–Australian palaeo-equatorial warm-climate 'province' (*Figure 1*) (Metcalfe, 2005).

A Late Cambrian age of the Chang Pung Formation has been proposed on the basis of trilobites and brachiopods: i.e. 1) the *Drepanura - Blackwelderia* Assemblage, considered as the lower faunal zone; and 2) the *Calvinella-Eoorthis* Assemblage, considered as the upper faunal zone (Depart, 1915, 1916; Mansuy, 1915, 1916; Kobayashi, 1944; Saurin, 1956; Dovjikov et al., 1965; Tinh, 1976, 2001; Thanh et al., 2006; Ngan et al., 2008). However, Huyen et al. (2007) suggest a Middle to Late Cambrian age based on trilobites, brachiopods, and acritarchs. The lower part of the succession is characterized by diverse Middle Cambrian fauna with *Tonkinella flabelliformis* (Pha Long area, Lao Cai), *Annamitia spinifera* (Vi Xuyen area, Thanh Thuy, Ha Giang), *Lingulella - Obolus*, Osagia (Pha Long area, Vi Xuyen) and *Baltisphaeridium* (Bac Quang area, Ha Giang). The upper section yields abundant Late Cambrian fossil assemblages in which 3 fauna development stages have been

differentiated, i.e. an early stage that is characterized by the development of *Drepanura premesnili*; a middle stage with the development of *Prochuangia mansuyi* and *Irringella taitzuhoensis* and a late stage characterized by the occurrence of *Prosaukia angulata* and *Calvinella walcotti*. The Chang Pung Formation lies conformably upon the Middle Cambrian Ha Giang Formation that has been observed in the Chang Pung and Thanh Thuy areas (Ha Giang Province) (Table 1).

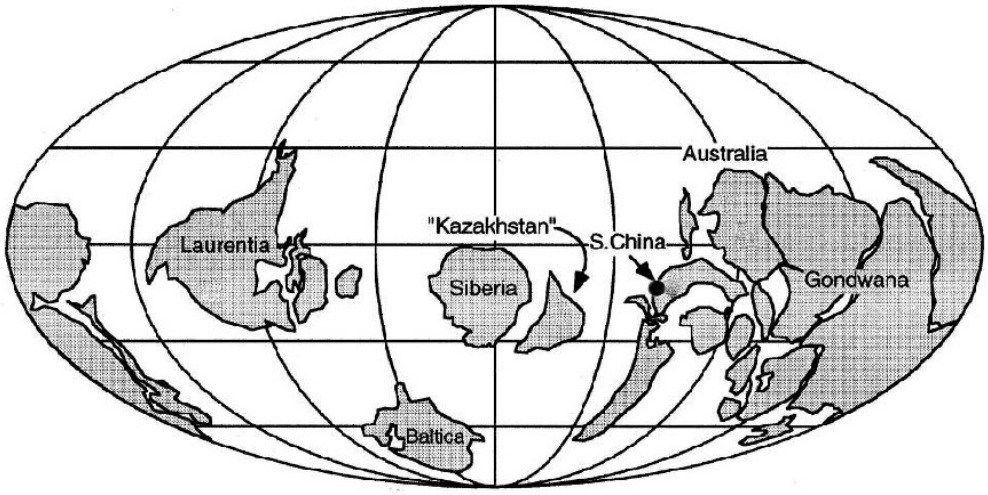

Figure 1. Paleogeographic map for the Late Cambrian (after Scotese and McKerrow, 1990) showing the approximate location of the South China plate with Dong Van Karst Plateau.

Table 1. *Lower Paleozoic stratigraphic units of Ha Giang area (after Thanh et al., 2006).*

Chronostratigraphiy		Lithostratigraphy	Main components
Ordovician	Early	Lutxia Formation	Limestone
Cambrian	Late	Chang Pung Formation	Limestone interbedded with argillaceous shale, siltstone and sandstone
	Middle	Ha Giang Formation	Sericite - quartz schist and limestone
Neoproterozoic	Early	Song Chay Group	Two-mica schist, muscovite schist, marble, tremolite marble

At the Lung Cu section, the lowest parts of the Chang Pung Formation have been not observed. Tran Huu Dan (Huyen et al., 2007) described the Lung Cu section in detail (*Figure 2*). The latter authors differentiated 13 members, namely (from bottom to top):

1. Grey, yellowish weathering, calcareous and argillaceous shale, siltstone. Thickness = 20m.

2. Black grey, thin-bedded brecciated limestone, argillaceous limestone, 8m thick.

3. Grey, yellowish weathering, calcareous and argillaceous shale, siltstone, marly shale, containing the trilobite *Damesella* sp. Thickness = 50m.

4. Ash - black grey, irregular medium bedded, oolitic limestone, argillaceous limestone, marly shale, 30m thick.

5. Ash-grey, yellowish weathering, calcareous and argillaceous shale, siltstone, marly shale, some argillaceous limestone, 90m thick.

6. Dark grey, regular medium bedded limestone, argillaceous limestone, oolitic limestone, brecciated limestone. Thickness = 250m.

7. Grey, yellowish weathering, marly shale, 10m thick.

8. Grey, regular medium bedded limestone, interbedded with some thin-bedded argillaceous limestone or grey marly shale. Thickness = 15m.

9. Greenish grey, yellowish to reddish weathering, calcareous and argillaceous shale, siltstone, marly shale, containing the trilobite *Prosaukia angulata*. Thickness = 120m.

10. Black grey, regular medium bedded, limestone, oolitic limestone containing many brachiopods such as *Dictyella* sp., *Saukia* sp. Thickness = 10m.

11. Greenish-grey, yellowing to pinkish weathering, calcareous and argillaceous shale, siltstone, containing the trilobite *Calvinella walcotti*. Thickness = 45m.

12. Grey, regular medium bedded limestone, 20m thick.

13. Grey, yellowish to pinkish weathering, marly shale, calcareous and argillaceous shale, siltstone, containing the trilobite *Calvinella walcotti*, *Eoorthi* sp., 18m thick.

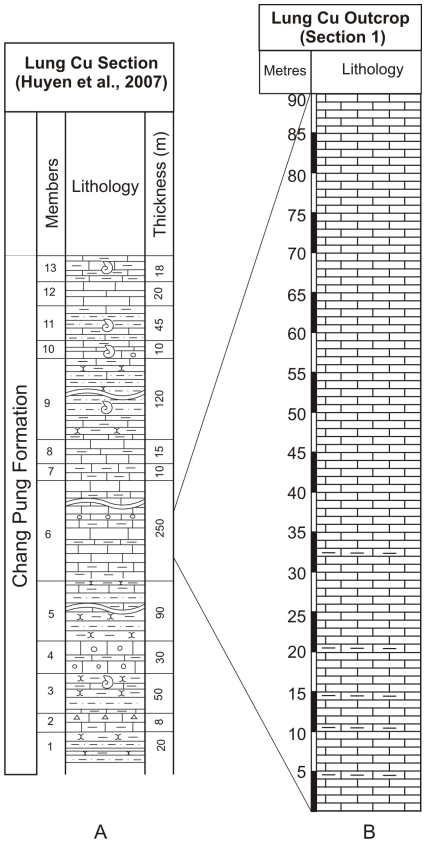

Figure 2. Stratigraphical log in the Lung Cu Section. (A) Stratigraphical log (after Huyen et al., 2007). (B) Stratigraphical log showing the studied intervals investigated in this study.

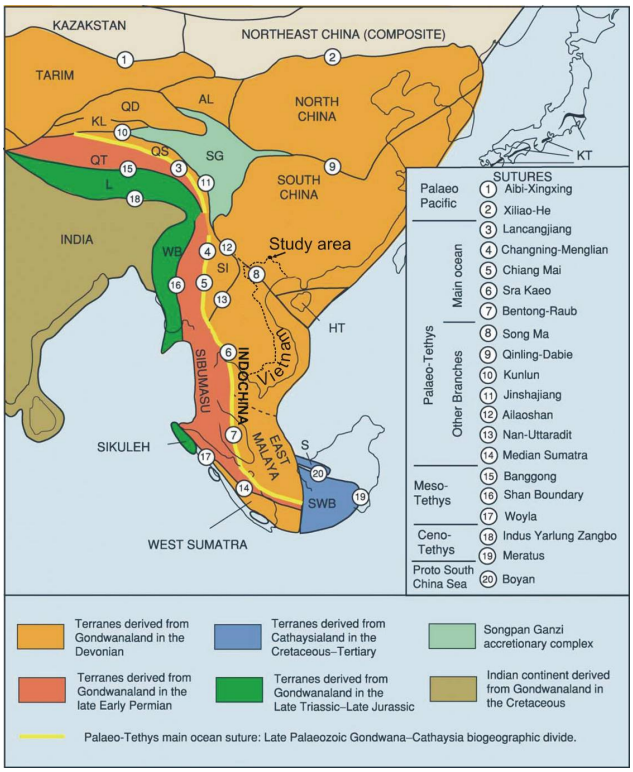

Figure 3. Distribution of the principal continental terranes and sutures of East and South-east Asia (modern topography) (modified after Mecalfe, 2005) with indication the approximate location of the study area. WB, West Burma; SWB, South West Borneo; S, Semitau Terrane; HT, Hainan Island terranes; L, Lhasa Terrane; QT, Qiangtang Terrane; QS, Qamdo-Simao Terrane; SI, Simao Terrane; SG, Songpan Ganzi accretionary complex; KL, Kunlun Terrane; QD, Qaidam Terrane; AL; Ala Shan Terrane; KT, Kurosegawa Terrane.

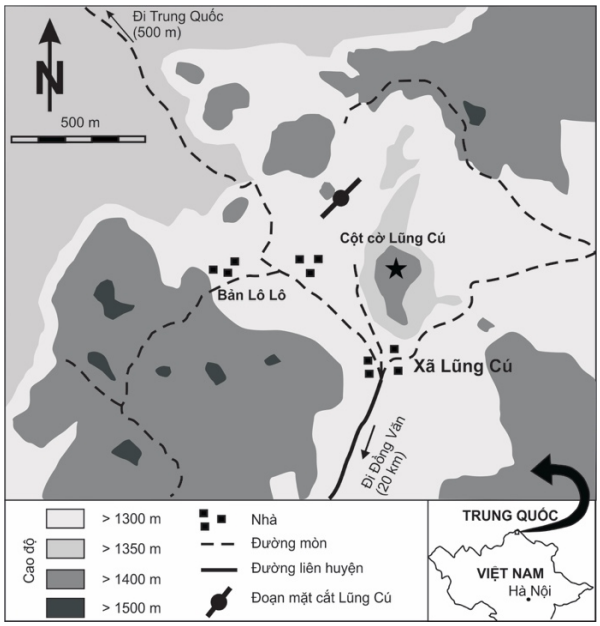

Figure 4. Map showing the locations of the Lung Cu outcrop of the Upper Cambrian carbonate succession at Lung Cu Village, Dong Van District, Ha Giang Province, Vietnam.

Photo 1. *The Lung Cu outcrop view from Lung Cu Flag Tower***.**

3. Methodology

3.1 Petrographic work

The present study of the lower part of Upper Cambrian carbonate succession of the Chang Pung Formation involved sampling from the measured stratigraphic section at Lung Cu outcrop. Eighty - two samples were collected from the measured section depending on the variations in colour, shape, and internal structures from bed to bed. Petrographic work followed the following a step-by-step work flow:

1. Rock slabs were produced from the samples collected in the field in order to obtain good surfaces to study the sedimentary features as well as diagenetic products. Polished and etched rock samples were digitally scanned to retain an image of the slabs before thin section preparation. Interesting areas for petrographic analysis were identified and thin sections were manufactured.

2. Observations at low and high magnifications allowed getting a general overview and detailed petrographic information from the thin sections (sedimentary and diagenetic features) with Zeiss microscopes.

3. Subsequently, a cathodoluminescence analysis was carried out. The presence of different cathodoluminescence colours proved especially useful to constrain the relative timing of crosscutting veins.

4. Subsequently, one half of each thin section was stained with Alizarin red-S and K-ferricyanide solution and again examined with transmitted light microscopy to differentiate dolomite from calcite and ferroan from non-ferroan carbonate minerals, respectively (cf. Dickson, 1966). If staining precedes cathodoluminescence (CL) observations, the original luminescence colour is often obliterated due to the presence of the stain coating. The latter thus should be removed before CL analysis can be carried out.

3. 2 Conventional microscopy

Rock samples were cut and polished. These samples were etched with HCl and stained with Alizarine Red S and K-ferricyanide (Dickson, 1966). This method is used to distinguish between calcite (pink coloured) and dolomite (no colouring) and their ferroan equivalents: ferroan calcite (purple coloured) and ferroan dolomite (turquoise). Thin sections were prepared from selected samples. A total of 82 thin sections were studied with plane polarised transmitted light to establish their sedimentary facies and to identify diagenetic phases and crosscutting relations. Incident light was used for the study of opaque phases.

3. 3 Cathodoluminescence microscopy

Cathodoluminescence microscopy was carried out on an adapted Technosyn Cold Cathodoluminescence device model 8200, Mark II, operating at 11–12 kV gun potential, 200–300 μA beam current, 0.05 Torr vacuum and 5 mm beam width. When the surface of thin section is bombarded with a high-energetic electron beam, visible light is emitted. This process is call cathodoluminescence. The wavelength and hence the colour and the intensity of the light emitted by a certain mineral phase depends on the operating conditions and the balance of the inhibitors and the activators. In carbonates, Mn^{2+} is an important activator while Fe^{2+} is an important inhibitor (Machel et al., 1991; Tucker, 1995).

The use of cathodoluminescence in sedimentological and diagenetic studies gives important information which is often hard to see by other petrographical means or can not be seen when using these other techniques. Cathodoluminescence is a tool to determine the relative timing of the diagenetic events of fracturing, stylolitisation and cementation by means of crosscutting relations. It can also help to unravel the cement petrography by distinguishing phases that were indistinguishable in transmitted light microscopy.

Cathodoluminescence microscopy also offers a possibility to differentiate between primary growth forms of the cement crystals, cements which have been affected by recrystallization, and other neomorphism processes.

4. Results and discussions

4.1 Petrographic interpretation

Carbonates have a special textural classification (Dunham, 1962) based on the presence or absence of lime mud or grain dominance. Textures range from grainstone, rudstone, and packstone (grain-supported) to wackestone and mudstone (mud-supported). Allochem is a term introduced by Folk (1959) to describe the recognisable 'grains' in carbonate rocks. This term is a collective term for mechanically deposited grains that, in most cases, have undergone transportation (Folk 1962). Carbonate grains include ooids, peloids, oncoids, cortoids, pisoids, fossils or pre-existing carbonate fragments. Grain types are paleoenvironmental proxies both for non-marine and marine carbonates (e.g. they reflect sedimentation environments, water energy levels, …).

4.2 Microfacies analysis

According to Burchette and Wright (1992), a carbonate ramp is a gently dipping sedimentary surface on the sea floor. The facies belts are controlled primarily by energy levels (fair-weather wave base and storm wave base), variations in ramp topography, and material transport by storms, waves and tides. Diagnostic criteria of inner, mid- and outer parts of ramps are discussed (Burchette and Wright 1992): The outer ramp is the zone below normal storm wave base. Water depths vary between tens of meters and several hundreds of meters; The mid-ramp is the zone between fair-weather wave base and the storm wave base. Water depths reach some tens of meters; The inner ramp comprises the euphotic zone between the upper shoreface (beach or lagoonal shoreline) and the fair-weather wave base. The sea floor is almost constantly affected by wave action.

The presence of carbonate grains and sedimentary structures observed in detailed information on the petrography data implied that the lower part of Upper Cambrian carbonate succession in the Lung Cu outcrop built up in the ramp carbonate were controlled by peritidal to mid-ramp in shallow-marine depositional environment. Eight significant facies types were distinguished according to lithology, texture, grain composition, and sedimentary structures (Photo 2). These facies types can be compared with the Microfacies Types of Carbonate Ramps scheme of Flügel (2004) following the carbonate ramp model.

Facies 1: Marl (~ RMF-type 2)

This facies is characterized by micritic limestone and argillaceous materials in very thin beds. The variation of bed thicknesses range from 0.5 to 1cm. Bedding normally consists of parallel beds, which are locally wavy beds.

Interpretation: The described parallel laminated beds and the presence micritic mudstone argillaceous materials can best be interpreted as RMF 2 indicating mid-ramp deposition in a quiet-energy regime.

Facies 2: Parallel bedded limestone (~ RMF-type 19)

This facies is characterized by micritic mudstone without fossils and parallel laminated beds varying from 2 to 10cm thick.

Interpretation: The described parallel laminated beds and the presence micritic mudstone can best be interpreted as RMF 19 indicating restricted lagoon deposition in a quiet-energy regime.

Facies 3: Wavy bedded limestone (~ RMF-type 22)

This facies is made up of mudstone with fossil fragments (such as trilobites and brachiopods) and interbedded bedding from 1 to 3cm, with parallel wavy beds. Fine sand-size detrital quartz grains occur in limestone.

Interpretation: The wavy bedded mudstones corresponding to RMF 22 are interpreted as peritidal deposits formed under low-energy conditions.

Facies 4: Oncoid- intraclast (~ RMF-type 21)

This facies is characterized by type B oncoids with intraclasts to lithoclasts, peloids, pisoids, cortoids and ooids.

These grains dominantly occur in wackestone to grainstones. The variation of bed thicknesses range from 0.3 to 1 m. Bedding normally consists of parallel beds, which are locally bioturbated.

Interpretation: Given the presence of type B oncoids, intraclasts to lithoclasts in parallel beds with local bioturbation, this facies correspond to RMF 21 and thus indicates a peritidal depositional environment with sedimentation under low-energy conditions. Oncoids often occur at the base of transgressive sequences formed in shallow low-energy environments (e.g. Wright 1983) and often mark maximum flooding surfaces.

Facies 5: Floatstone – intraclast – extraclast (~ RMF-type 21)

This facies is composed of floatstones/packestones with intraclasts, extraclasts and pebbles. Thin parallel beds are 4 to 5cm thick, with presence of bioturbation/erosion. Some intervals beds show wave ripples.

Interpretation: Based on the presence floatstone with pebbles and the wavy beds, these sediments are interpreted as RMF 21 indicating peritidal setting deposited under high-energy conditions.

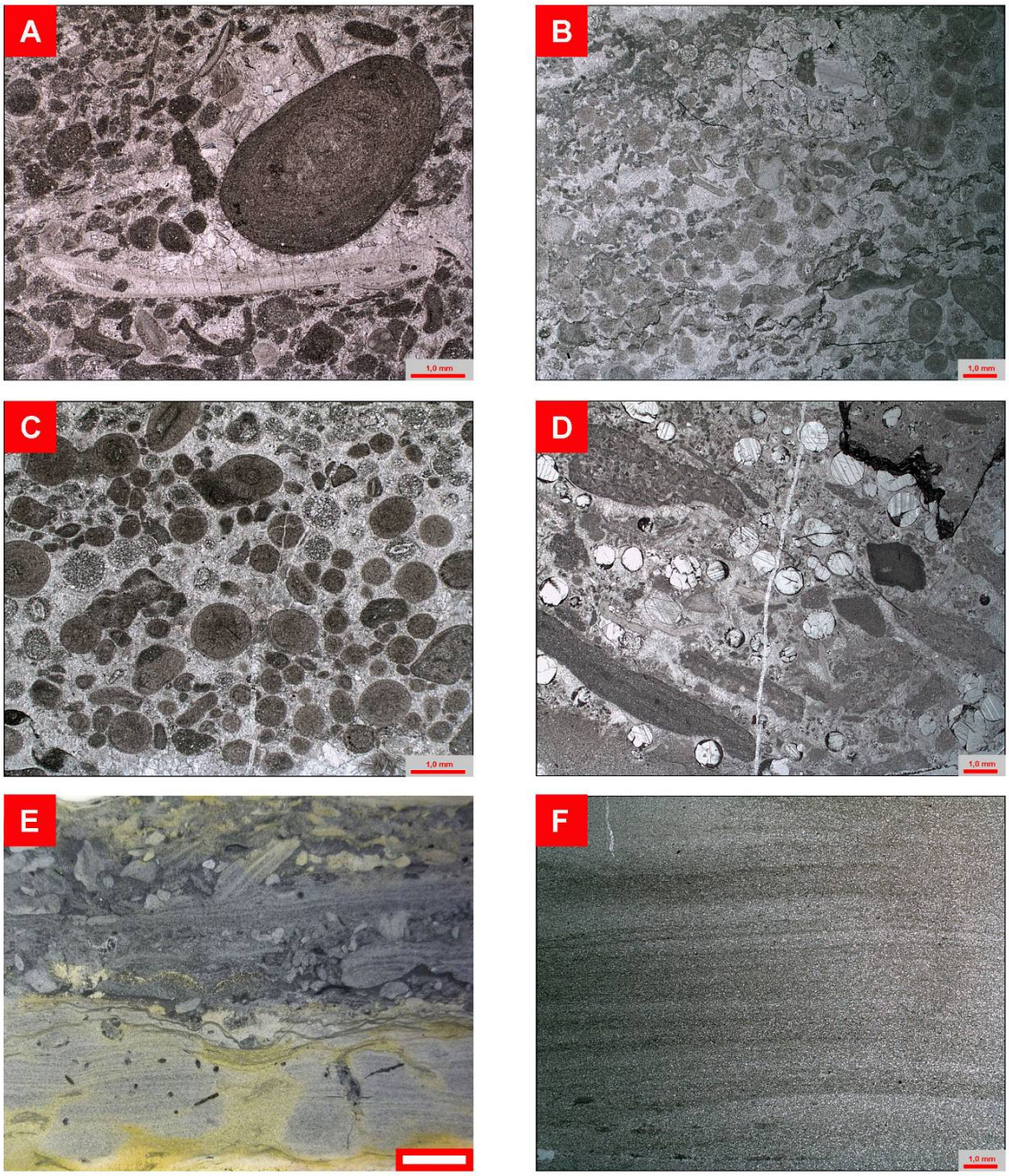

Photo 2. *Plate showing the microfacies of the Lung Cu outcrop carbonate succession***.** (A) Oncoid-intraclasts (Facies 4). (B) Ooid-bioclast-oncoid (Facies 7). (C) Ooid-lithoclast (Facies 8). (D) Bioclast-lithoclast-ooid (Facies 6). (E) Floatstone-intraclast-extraclast (Facies 5). (F) Mudstone (Facies 3)

Facies 6: Bioclast-lithoclast-ooid (~ RMF-type 27)

This facies consists of wackestones to grainstones with bioclasts such as sponges and trilobite. They are composed of some amounts of ooids and lithoclasts. The ooids have calcite and dolomite crystal nuclei and a thin micritic cortex. Bed thicknesses range from 1 to 3cm. Bedding is commonly

parallel, but some intervals show wave ripples or cross-bedding.

Interpretation: This facies is interpreted to be similar as RMF 27 indicating shoal depositional sedimentation conditions in a high-energy regime.

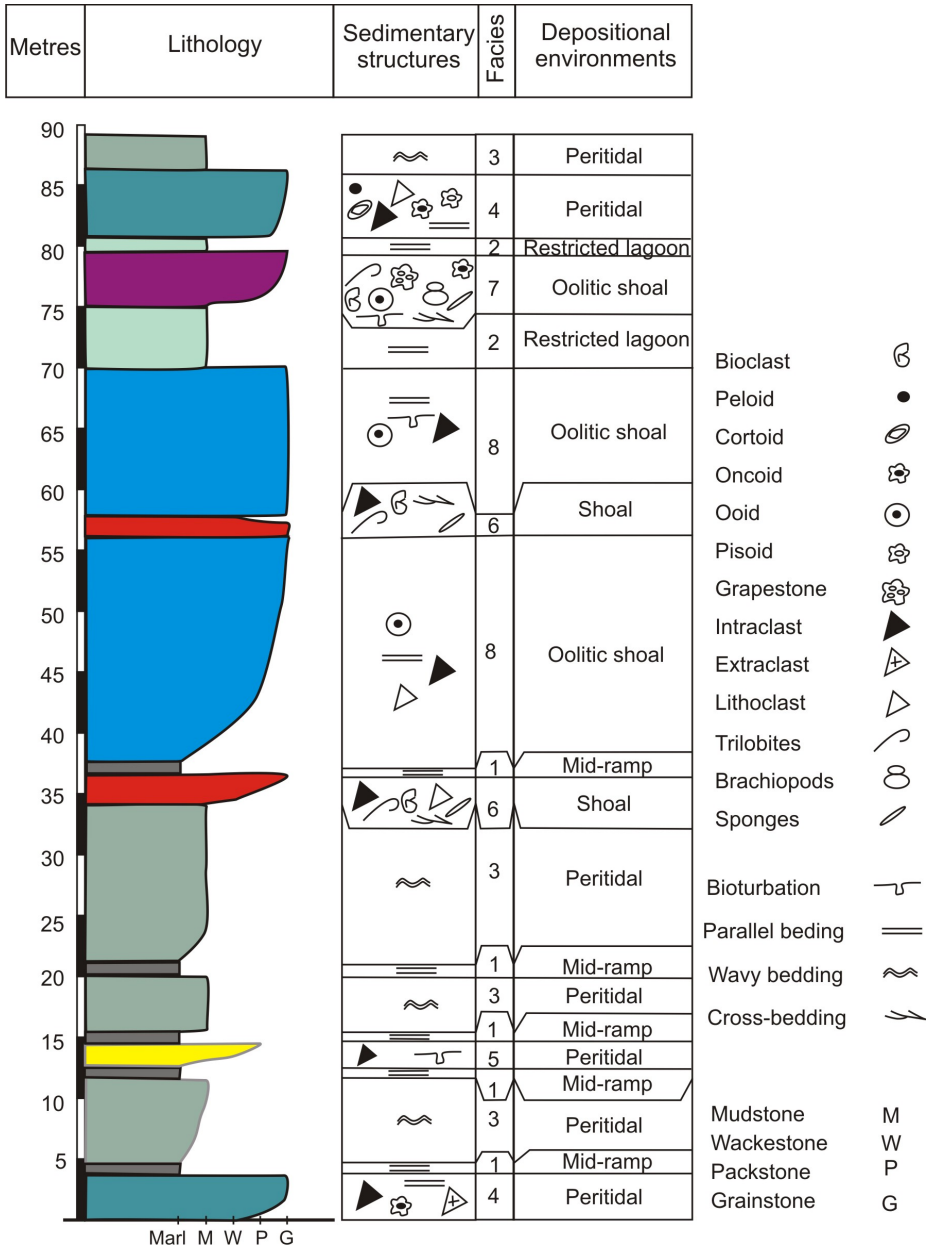

***Figure 5**. Sedimentological log and paleoenvironmental interpretation of the Lung Cu outcrop.*

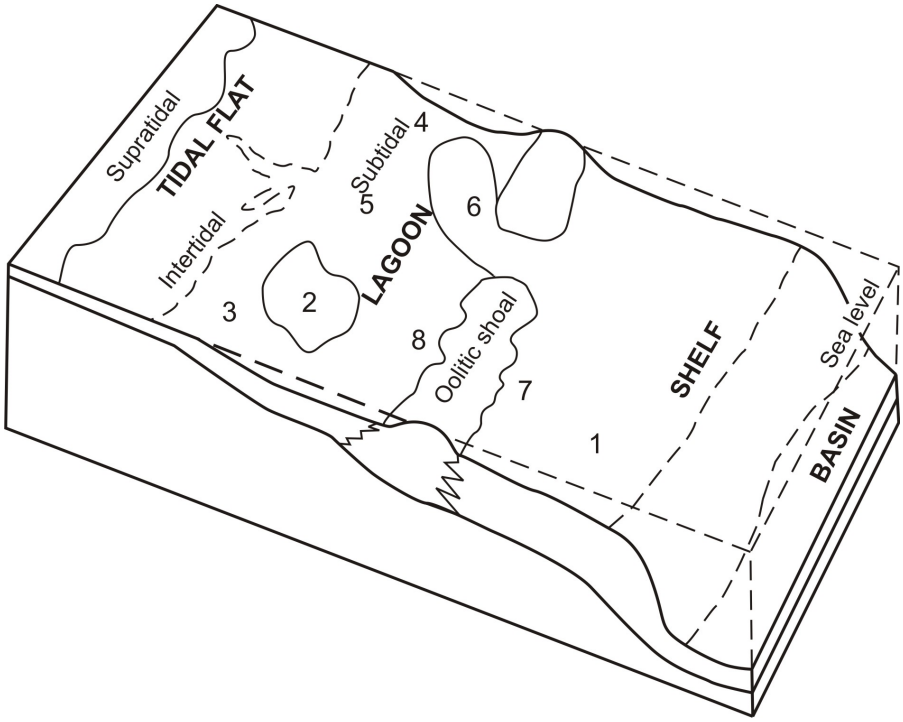

Figure 6. *The ramp carbonate model for the Lung Cu outcrop carbonate succession characterized by the presence of carbonate grains deposited in peritidal to mid-ramp in shallow-marine* depositional environment*. 1- Marl (Facies 1); 2- Parallel bedded limestone (Facies 2); 3- Wavy bedded limestone (Facies 3); 4- Oncoid- intraclast (Facies 4); 5- Floatstone-intraclast-extraclast (Facies 5); 6- Bioclast-lithoclast-ooid (Facies 6); 7- Ooid-bioclast-oncoid (Facies 7); 8- Ooid-lithoclast (Facies 8).*

Facies 7: Ooid-bioclast-oncoid (~ RMF-type 29)

This facies consists of wackestones to grainstones with concentric and radial ooids with variable sizes, asymmetrical and eccentric ooids, grapestones within some ooids, lithoclasts and type A oncoids. These strata are enriched in bioclast fragments from trilobites, brachiopods, sponges, etc... Beds thicknesses vary from 0.5 to 1m. Bedding is commonly parallel, but some intervals show, wavy or cross-bedding.

Interpretation: The described ooids, type A oncoids and bioclasts and their cross-bedding can be interpreted as RMF 29 indicating oolitic shoals deposited under high-energy conditions. The presence of type A oncoids with fossils may indicate regressive conditions (Fügel, 2004).

Facies 8: Ooid-lithoclast (~ RMF-type 30)

This facies is characterized by pack-stone to grainstone with irregular ooids, distorted ooids, pisoids, lithoclasts and grapestones within some ooids. Ooids are poorly sorted and the thickness of the concentric layers is equal or greater than half the diameter of the ooid. The thickness of beds is variable and varies from 0.4 to 1m, with thinnest beds measuring 1–5cm. Bedding are commonly parallel.

Interpretation: They are interpreted as RMF 30 indicating oolitic shoals deposited under low-energy conditions. Grainstones predominantly consisting of aggregate grains are characteristic parts of platforms formed during sea level highstand phases (Flügel, 2004).

4.2 Diagenesis

The term early diagenesis refers to diagenesis occurring immediately after deposition or immediately after burial (Berner 1980). The most important processes occurring in early diagenesis of carbonates are micritization, cementation, dissolution, dolomitization and dedolomitization and compaction. Studies of thin sections are of paramount importance in recognizing diagenetic environments and determining paragenetic sequences in carbonate rocks. Success in reconstructing the diagenetic history depends heavily on the ability to recognize the primary crystal shapes of the cements, stylolites, veins, dolomite and their crosscutting relationships.

4.2.1 Micritization

Micritization is a process whereby the margins of carbonate grains or the total volume of grains are replaced by crypto- or microcrystalline carbonate crystals (Flügel, 2004). The term micrite envelope was first used by Bathurst (1964) in the study of syngenetic and early diagenetic changes affecting modern skeletal grains. The term refers to a thin, non-laminated coating of very fine micrite around carbonate grains, particularly skeletal grains or ooids. The strong micritization indicate the existence of a very shallow sea.

4.2.2 Cementation

Base on their morphology and cathodoluminescence characteristics, at least four distinct types of early diagenetic calcite cement, such as radiaxial fibrous, granular, blocky, and syntaxial calcite overgrowth cements, have been recognised.

Radiaxial fibrous cements

Radiaxial fibrous cement formed between large lithoclast grains (***Photo 3***A, B, C, and D). These cements consist of large, often cloudy and turbid, inclusion-rich calcite crystals with undulose extinction. Their length usually varies from 30 up to 900 µm. Crystal length to width ratio grades from 1:3 to 1:10. Cathodoluminescence colours of these cements in general are brown to orange. Within each subcrystal that diverges away from the substrate an opposing pattern of distally-convergent optic axes occurs, caused by a curvature of cleavage and twin lamellae (Bathurst 1959, 1982; Kendall and Tucker 1973; Kendall 1985). These cements are interpreted to be syndepositional marine, shallow-burial marine (Halley and Scholle 1985), or subaerial meteoric in origin.

Granular cements

Granular cements are characterised by relatively equidimensional pore-filling small crystals (*Photo 3*E, F). The size of the calcite crystals usually varies from 80 up to 300µm. Distinction between other types of cement is based on their uniform crystal size or gradual increasing crystal size towards the pore center. These crystal phases can also originate from recrystallization of pre-existing cements or micrite. The cement displays a brown to orange luminescence under cathodoluminescence. These cements are assumed to be formed in meteoric-phreatic and burial environments, and eventually in a meteoric vadose setting (Flügel, 2004).

Blocky cements

Blocky cements consist of medium to coarse crystalline crystals without a preferred orientation (*Photo 4*A, B). These crystal sizes vary from100 to 400 µm. Crystal sizes increases towards the centre of a pore. Cathodoluminescence colours of this cement type vary between brown and orange. These blocky textures can also originate from recrystallization of preexisting cements, but then the gradual increase in crystal size is non existent. This type of cement is assumed to have formed in a meteoric (meteoric phreatic and vadose) and burial environments (Flügel, 2004).

Syntaxial calcite overgrowth cements

Syntaxial calcite overgrowth cements are substrate-controlled overgrowth around a host grain made by a mono crystalline grain, such as a crinoid for example (*Photo 4*C, D). Overgrowth cementation formed in

crystallographic lattice continuity with their substarte. Color of the skeletal grain is grey and the overgrowth cement is transparent. Syntaxial calcite overgrowth cement is typical for near-surface marine, vadose-marine and meteoric-phreatic environments (Flügel, 2004).

At least four distinct types of early diagenetic cement occur within the Lung Cu outcrop carbonates. These early diagenetic cements include (1) radiaxial fibrous, (2) granular, (3) blocky, and (4) syntaxial calcite overgrowth cements. Radiaxial fibrous cement formed between large lithoclast grains. These cemented forms are large, often cloudy and turbid, inclusion-rich calcite crystals with undulose extinction. These are the characteristics of first generation cements in many limestones of syndepositional marine, shallow-burial marine (Halley and Scholle 1985), or subaerial meteoric origin. A second-generation cement of granular cements are characterised by relatively equidimensional pore-filling small crystals. These cements can also originate from recrystallization of pre-existing cements. They formed in meteoric vadose, meteoric-phreatic and burial environments (Flügel, 2004). The third type of cement is blocky cement, which generally completely fills the intergranular pores with medium to coarse grained crystals. These cements are generally located in the centre of the pores without a preferred orientation. Blocky textures can also originate from recrystallization of preexisting cements. This type of cements formed in meteoric (meteoric phreatic and vadose) and burial environments (Flügel, 2004). The fourth type of cement observed is syntaxial calcite overgrowth cements on coated grains. The overgrowth shows strongly preferred orientation in optic continuity with the coated grains nucleus. Coating of micrite on the grains and in the outer pores obliterates the development of syntaxial calcite overgrowth cement. Textural evidence suggests that overgrowth is contemporaneous with early marine cements and the two show interference effects reflecting a competitive growth. Some studies relate the overgrowth to the freshwater diagenetic environment (e.g. Halley and Harris, 1979; Land, 1970; Jacka and Brand, 1977; Meyers, 1978; Longman, 1980). This type of cement is characterised by near-surface marine, vadose-marine and meteoric-phreatic environments (Flügel, 2004).

4.2.3 Dissolution

Paleokarsts

Paleokarsts features consist of millimeter- to several millimeter-sized void or fissures, oriented vertically, horizontally or oblique with respect to bedding, and filled with internal sediment, consisting of black mudstone, quartz and plagioclase crystals without fossils (*Photo 7*). They occur in pack- to grainstones containing oncoids, intraclasts to lithoclasts, radiaxial fibrous and spar cements, veinlets, dolomite and dedolomite crystals, geopetal infill. The dolomite clasts in the cavity suggest that the dolomitization associated with the unconformity pre-dated the cavity infill, so that such dolomitization was early and took place during the phase of sea-level fall, probably through mixing water diagenetic processes. These paleokarst features formed during subaerial exposure with dissolution in a meteoric-vadose, marine-vadose or meteoric-phreatic realm (Flügel, 2004). Most meteoric paleokarsts have originated where shallow marine limestones became subaerially exposed by a fall in relative sea level (Wright and Smart, 1994).

Evidence of dissolution is the presence of paleokarsts filled with internal sediment, consisting of black fine mudstone, quartz and plagioclase crystals without fossils. Paleokarsts often cut radiaxial fibrous and spar cements. Paleokarst is formed during dissolution diagenesis under meteoric - vadose, marine - vadose and meteoric-phreatic conditions after cementation process.

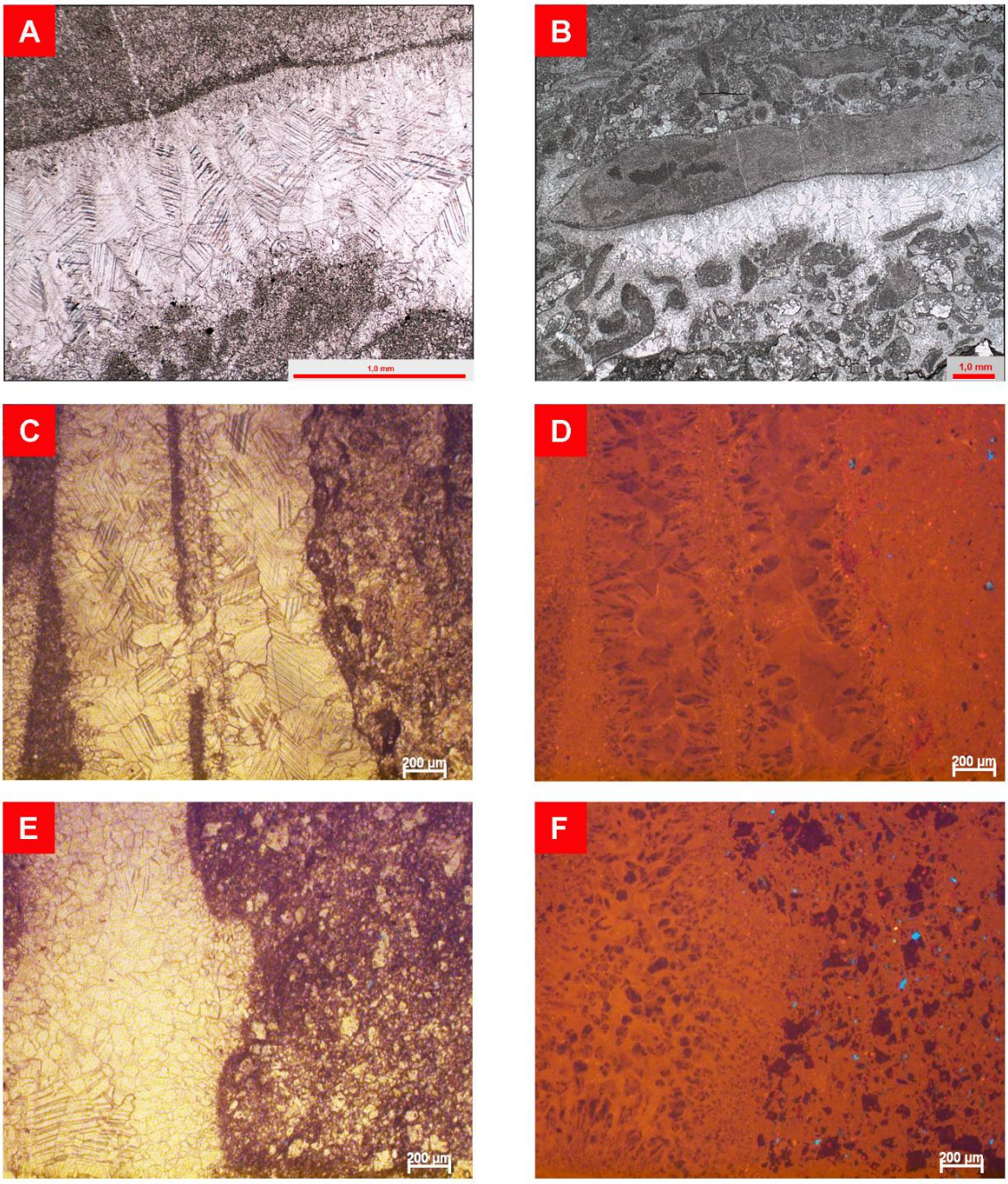

Photo 3. *Fig. 12. Transmitted light and cathodoluminescence microphotography from calcite cement. (A, B, C and D) Radiaxial fibrous calcite cements. Packstone: intraclasts to lithoclasts, spar calcite cements and veinlets. (E and F) Granular cements. Grainstone: dolomite (red) and quartz (blue).*

4.2.4 Dolomitization and dedolomitization

Dolomite is a calcium magnesium carbonate mineral ($CaMg(CO_3)_2$). Three broad categories of dolomitization model are currently available for the interpretation of ancient dolomites, namely marine related (with pure seawater, evaporative seawater

and seepage-reflux), mixing-zone and burial models.

Based on their morphology and distribution two types of dolomites in the Lung Cu outcrop (Section 1) can be differentiated, namely types 1 and 2 dolomites. The dolomite texture described below is according to the classification model of Sibley and Gregg (1987).

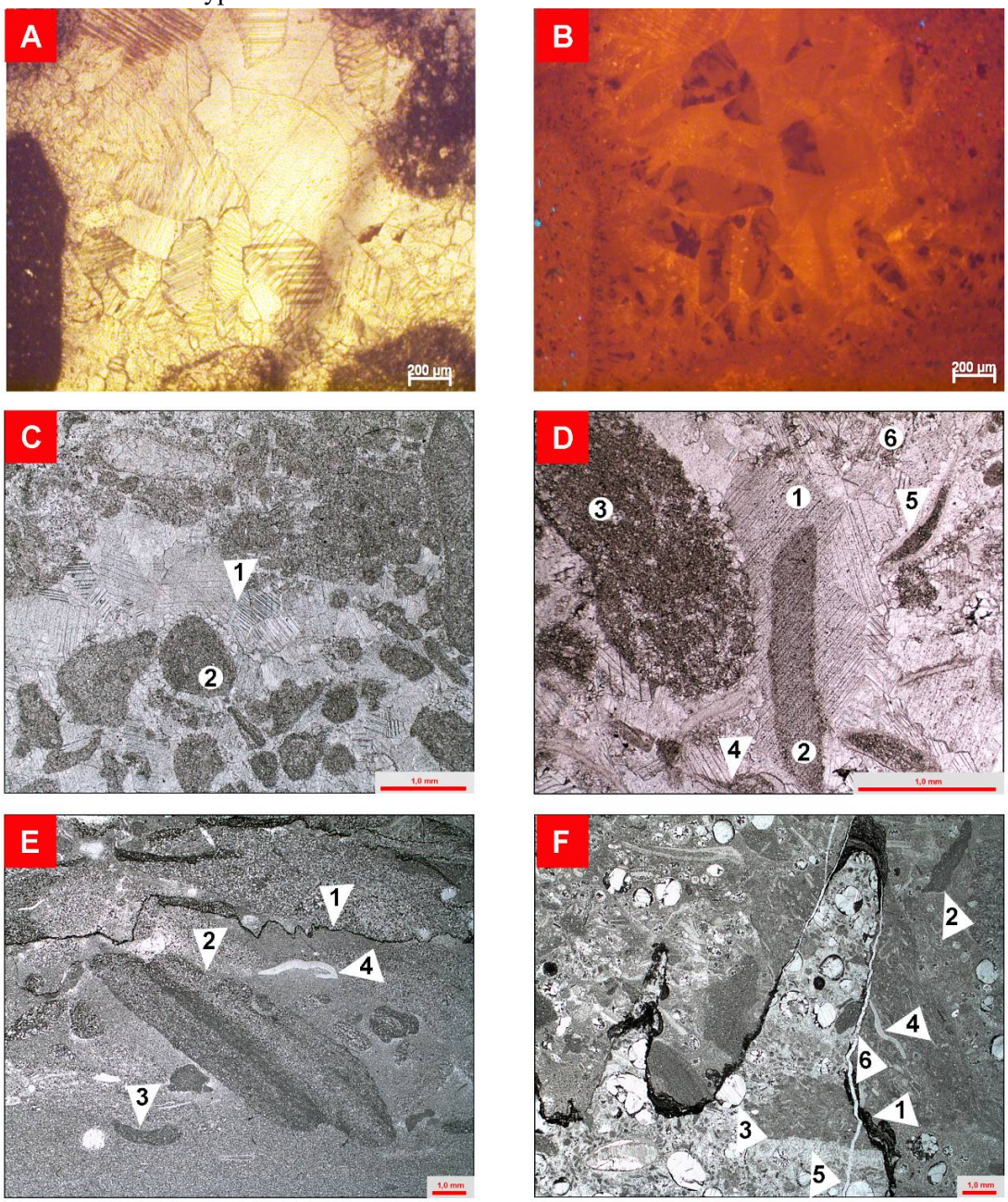

Photo 4. *Fig. 13. Transmitted light and cathodoluminescence microphotography from calcite cement and stylolite. (A and B) Blocky cements in grainstone with sector zonations in B. (C and D) Syntaxial calcite overgrowth cements (1). Grainstone: intraclasts (2) to lithoclasts (3), trilobite (4), sponges (5), and granular cements (6). (E) Small amplitude stylolite (1).*

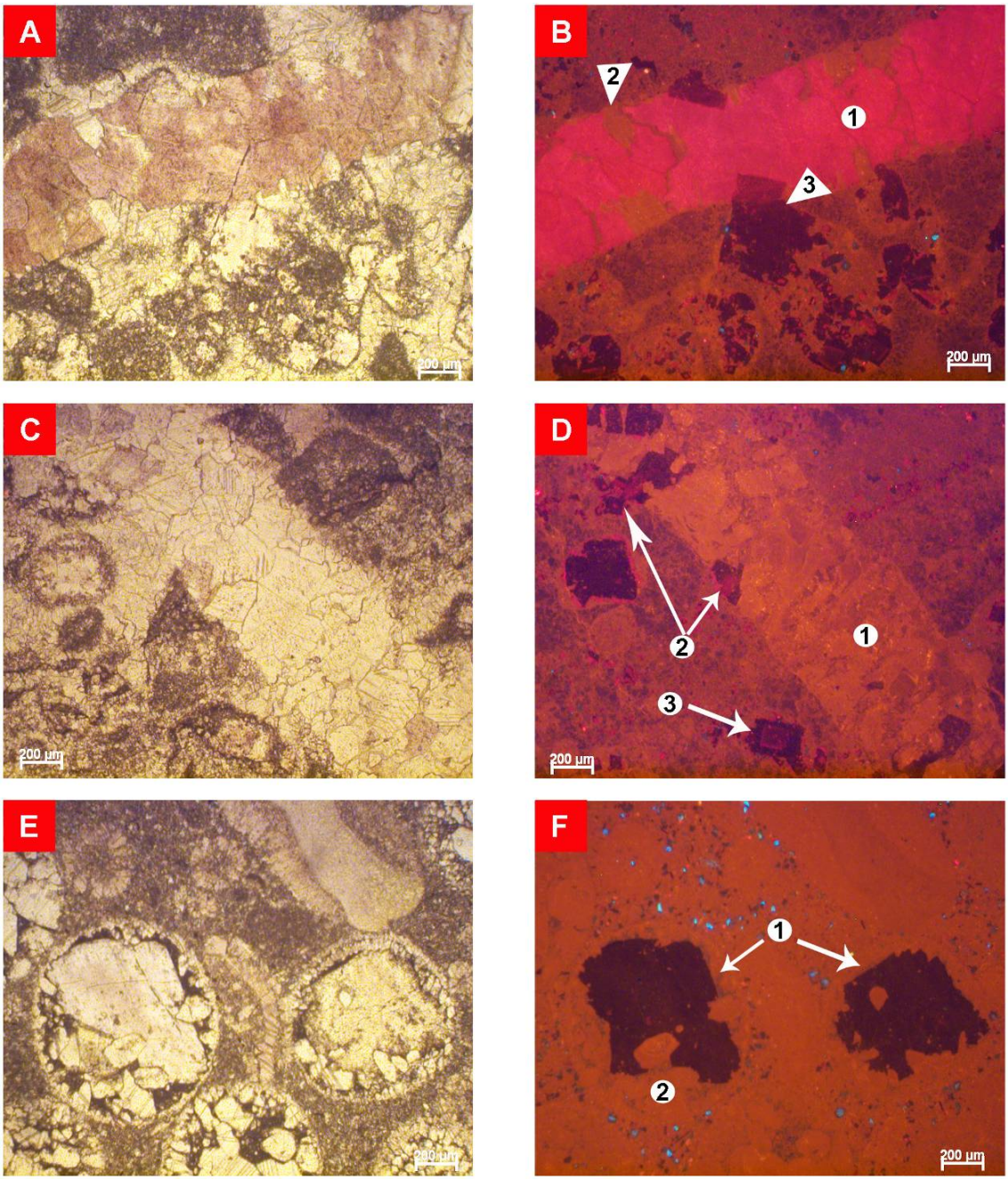

Photo 5. *Fig. 14. Transmitted light and cathodoluminescence microphotography from veinlets and type 2 dolomites. (A and B) Calcite (2) and type 2 dolomite (3) inside the pink veinlet (1), and quartz (blue). (C and D) Type 2 dolomite (2) insides the brown veinlet (1), and dedolomite (3). (E and F) Type 2 dolomites (1) and calcites (2) inside the ooids, and quartz (blue).*

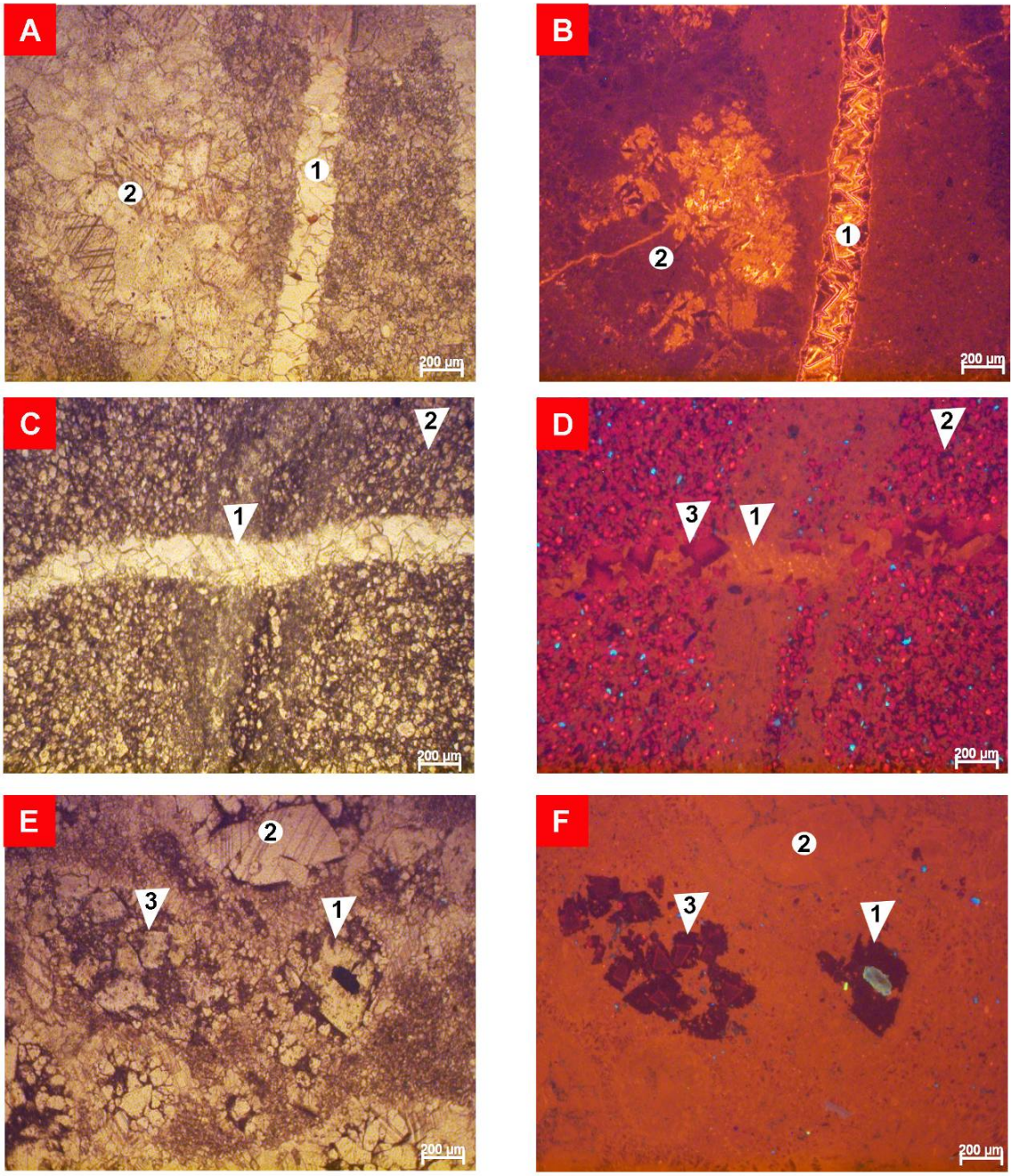

Photo 6. *Fig. 15. Transmitted light and cathodoluminescence microphotography from veinlets, calcites (yellow to orange) and dolomites (red). (A and B) Red-violet veinlet (1) and blocky cements (2) in grainstone. (C and D) Type 1 dolomites (2) are tiny crystals (10–30 µm in size), type 2 dolomites (50–150 µm in size) (3) inside the brown veinlet (1), and quartz (blue) in grainstone. (E and F) Type 2 dolomites (1) and calcite (2) inside the ooids, dedolomites (3) and quartz (blue) in grainstone.*

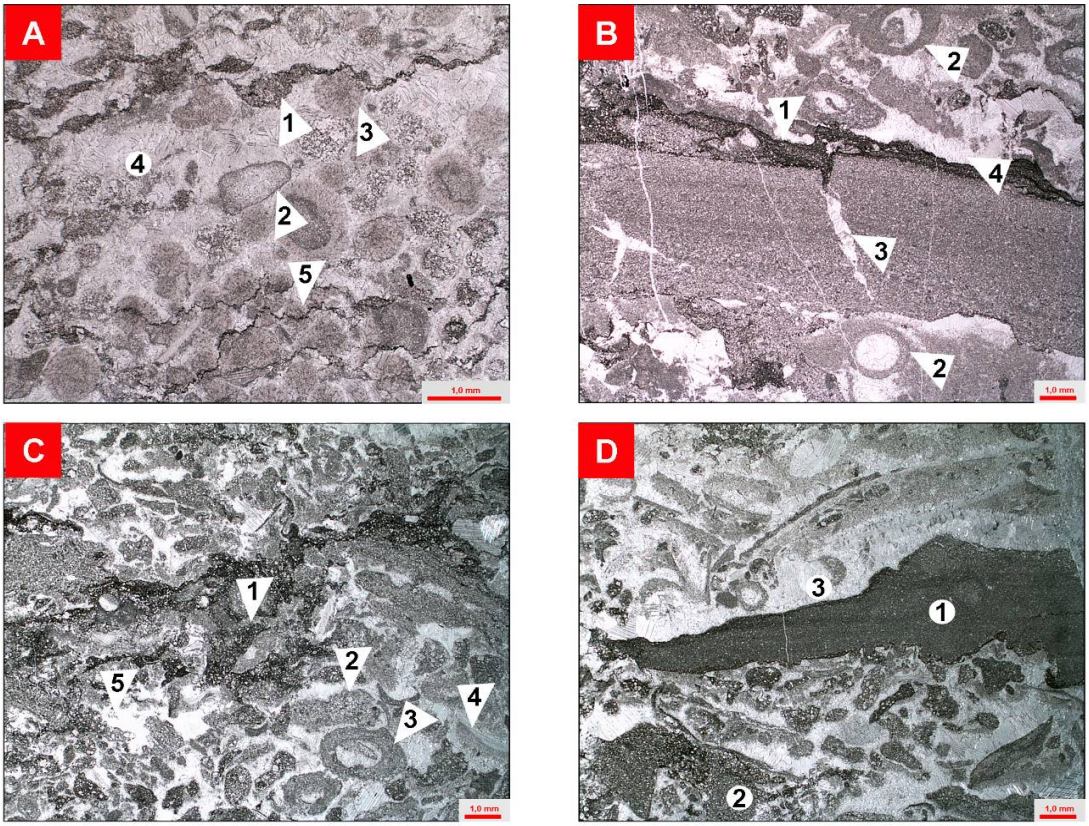

Photo 7. Fig. 16. Transmitted light microphotography of paleokarst infill present in pack- to grainstones. (A) Paleokarst (1) filled by micrite calcite, lithoclasts (2), ooids (3), spar cements (4) and small amplitude stylolites (5). (B) Paleokarst (1) filled by quartz and plagioclase crystals, ooids filled by spar cement (2), fissures filled by spar cement (3) and spar cements (4). (C) Paleokarst (1) filled by quartz and plagioclase crystals, lithoclasts (2), oncoids filled by spar cement (3), syntaxial calcite overgrowth cements (4) and spar cements. (D) Paleokarst (1) filled by black mudstone, lithoclasts (2) and spar cements.

Type 1 dolomite consists of fine small crystalline phases (10–30 μm), which are occasionally planar- e (euhedral) dolomite rhombs (*Photo 6*C). These dolomites thus have a characteristic "sugary" texture. The intensity of dolomitization varies from isolated rhombs floating in the micritic matrix to the development of an idiotopic mosaic texture. In CL analysis, type 1 dolomites commonly reveal zonation (different shades of red for the outer zones with the core displaying a brighter red CL, ***Photo 6***D). Macroscopically the existing type 1 dolomites often consist of light-grey to grey phases occurring in dark-grey pack- to grainstone. The type 1 dolomites display an irregular distribution, which is discordant to bedding. According to Sibley and Gregg (1987) and Warren (2000), this indicates precipitation temperatures below 50–60 °C (i.e., early stage formation during shallow burial).

Type 2 dolomite is coarsely crystalline (50–150 μm in size) possessing planar-e (euhedral) or planar-s (subhedral) dolomite rhombs (*Photo 5*E, F and *Photo 6*C, D, E, F). The intensity of dolomitization varies from idiotopic to hypidiotopic mosaic texture. This

commonly exhibit a similar zoned CL pattern as type 1 dolomites, consisting of a brighter core surrounded by a dark red rim. This texture is reported to have formed at temperatures superior to 50–60 °C (i.e., late precipitation during deeper burial) (Sibley and Gregg, 1987 and Warren, 2000). Tucker and Wright (1990) suggested that Mg^{2+} ions are more strongly hydrated in seawater than Ca^{2+} ions and they are also involved in ion pairing. This means that there are fewer Mg^{2+} ions available for reaction and that Ca^{2+} ions more easily enter growing Ca-Mg carbonate crystals. Once incorporated onto a growing crystal surface, the hydrated Mg^{2+} ions then provide a barrier for the CO_3^{2-} anions. The hydration of Mg^{2+} is more easily overcome through crystal growth at higher temperature, so that this is a factor often cited in favour of burial dolomitization. Type 2 dolomites were not macroscopically recognized, but these can be found in any stratigraphic position of the measured sections by thin sections. These dolomites occasionally occur inside ooids or veinlets. Dolomite 2 occurred after compaction.

Dedolomite consists of rhomb-shaped pores that are either completely filled with calcitic microsparite (cements) or, more frequently, consisting of a thin, rhomb-shaped crystalline rim with a micritic fill (*Photo 5*D and *Photo 6*E, F). Most rhombs have one or more of their corners missing. In (former) crystal geometry and size, all dedolomites correspond to type 2 dolomites. Dedolomite appears inside dolomite crystals of type 2. Obviuosly dedolomitization occurred after dolomitization type 2. Most authors consider dedolomitization to be a near surface process related to weathering (Nader et al., 2008). Laterally continuous dedolomitized horizons, therefore, may indicate the presence of unconformities (Brown and Friedman 1970). Guo et al. (1996) demonstrated that Ordovician dedolomites, characterized by low Fe^{2+} contents and depleted $\delta^{18}O$ values, occurred during uplift, subaerial exposure and karstification through the circulation of meteoric water within porous dolostones. The release of Fe^{2+} into the oxidized (near-surface) solution upon dedolomitization invokes the precipitation of iron oxides/hydroxides in some places within the karstic conduits/networks.

Two phases of dolomitization and one phase dedolomitization occur in this study. The presence of type 1 dolomite with small crystalline and sugary texture inside paleokarst is evidence of dolomitization 1. This stage occurred after dissolution. Evidence of the second phase is the presence of type 2 dolomite with coarsely crystalline inside ooids or veinlets. This dolomitization 2 phase took place after compaction 1. Dedolomite appears inside dolomite crystal of type 2 dolomite. This indicates that dedolomitization occurred after dolomitization 2.

4.2.5 Compaction

4.2.4 Stylolites

Stylolites are irregular, zigzag and suture-like contacts. Amplitudes of stylolites may range from < 1 mm to 5 mm (*Photo 4*E, F). Stylolites cross the whole rock, intersecting grains and cement. Stylolites are usually parallel or subparallel to bedding of rock. Microstylolites occur at burial depths as shallow as 90 m (Shlanger, 1964), stylolites as shallow as 60 m (Dunnington, 1967). They formed by chemical compaction under burial conditions (Flügel, 2004).

4.2.5 Veinlets

Veinlets are small joints filled with coarse crystalline calcite and/or dolomite phases. Veinlets widths range from millimeters to over a centimeter. Vein walls are normally subparallel, planar or irregular undulating. Based on their morphology, cathodoluminescence color and crosscutting relationship characteristics three types of veinlets can be differentiated, such as brown, red-violet and pink veinlets (***Photo 4***, ***Photo 6***). Misik (1966) distinguished veinlets formed by tension from those formed by compression using infilling characteristics and relationship with microstylolites. The latter author drew attention to a specific veinlet type characterized by a set of thin parallel veinlets separated by micrite and

believed to have been formed by repeated cracking and recrystallisation, i.e. crack – seal mechanisms (Misik 1998).

Evidence of compaction is pronounced in the Lung Cu Outcrop, which includes stylolites and distorted ooids. Two phases of compaction are observed. Evidence of the compaction 1 phase is the presence of distorted ooids, veinlets and small amplitude stylolites across the whole rock, and dolomite 1 crystals. This phase formed during chemical compaction under burial conditions after dolomitization 1. The presence of lager amplitude stylolites across the whole rock, dolomite 2 crystals, ooids and cements is evidence of a compaction 2 phase during chemical compaction under burial conditions after dolomitization 2. Relationship between the compaction 2 phase and the dedolomitization is not observed.

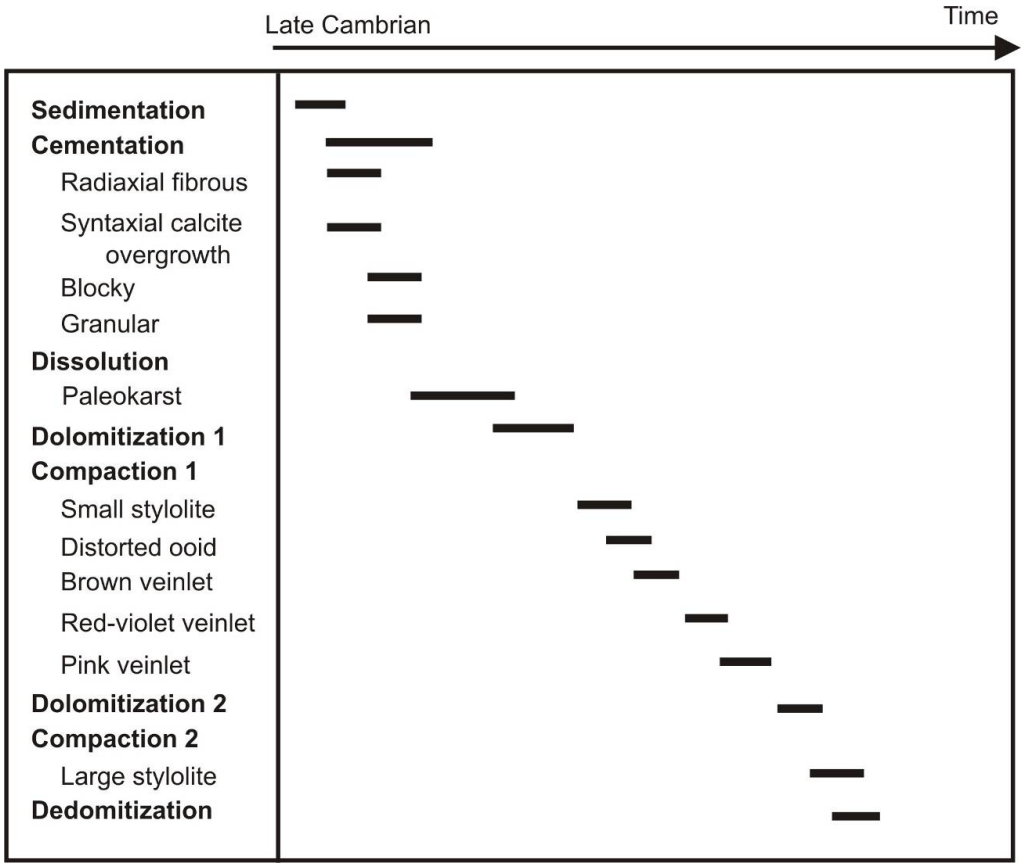

Figure 7. *Schematic illustration of the paragenetic sequence in the study area.*

6. Conclusions

In this manuscript the sedimentological characteristics of the carbonate succession in the Lung Cu outcrop are presented and a first attempt to reconstruct the paleoenvironmental conditions is given.

These sediments are composed of an alternation of oolitic pack- to grainstones, oncolite pack- to grainstones, intraclast to lithoclast grainstones, wackestone and mudstones with abundant bioturbation. Eight significant facies types were distinguished according to lithology, texture, grain composition, and sedimentary structures. The following facies were identified:

Facies 1 is characterized by micritic limestone and argillaceous materials in very thin beds, which indicates mid-ramp deposition in a quiet-energy regime.

Facies 2 is characterized by micritic limestone with parallel laminated beds, which formed in a restricted lagoon deposition in a quiet-energy regime.

Facies 3 is made up of micritic limestone with parallel wavy beds, which was deposited in peritidal deposits formed under low-energy conditions.

Facies 4 is made up of oncoids, intraclasts to lithoclasts, peloids, pisoids cortoid, ooids and bioturbattion, and reflects sedimentation in a peritidal depositional environment with sedimentation under low-energy conditions.

Facies 5 consists of intraclasts, extraclasts and pebbles, deposited in peritidal setting deposited under high-energy conditions.

Facies 6 is ooids, lithoclasts, bioclasts with sponges and trilobites, which indicates shoal depositional sedimentation conditions in a high-energy regime.

Facies 7 consists of concentric, radial and asymmetrical and eccentric ooids, bioclasts with trilobites, brachiopods, sponges, lithoclasts and oncoids, which is characteristic for deposition in oolitic shoals under high-energy conditions.

Facies 8 is characterized by ooids with variable sizes, distorted ooids, oncoids, pisoids, lithoclasts, grapestones, which likely formed in oolitic shoals deposited under low-energy conditions.

Sedimentary interpretations for these lithologies suggest that these facies of the carbonate succession in the Lung Cu outcrop correspond to the sediments of a peritidal to mid-ramp in shallow-marine setting.

Different diagenetic products have been identified and allow to work out a paragenetic sequence for the Lung Cu outcrop including cementation, dissolution, dolomitization and dedolomitization and compaction. Four types of early diagenetic cements have been recognized, namely radiaxial fibrous, granular, blocky, and syntaxial calcite overgrowth cements. Radiaxial fibrous cements are the characteristics of first generation cements in many limestones of syndepositional marine, shallow-burial marine or subaerial meteoric origin. A second-generation cement of granular cements originates in meteoric vadose, meteoric-phreatic and burial environments. The third type of cement is blocky cements formed in meteoric (meteoric phreatic and vadose) and burial environments. Syntaxial calcite overgrowth cements are the final generation cements originate from near-surface marine, vadose-marine and meteoric-phreatic environments. The presence of paleokarsts at the top of Lung Cu outcrop originated when the shallow marine limestones became subaerially exposed by a fall in relative sea level.

Acknowledgement

We thank Dang T. Huyen, Tran H. Dan, Dinh C. Tien, Nguyen V. Hien, (Vietnam Institute of Geosciences and Mineral Resources) for their help in fieldwork. This petrographic-stratigraphic research was financially supported by the “Integrated capacity building through research-based geopark development in N.E. Vietnam” (Geopark) project (2007 - 2012) (FWO discipline code(s): S214/S280/S285/P470/P510/P460) and the "Research on geological heritage sites and proposals of building geoparks in the northern area of Viet Nam", led by Dr. Tran Tan Van (KC.08/06-10). This study was financially supported by the Vietnamese project ‘Stratigraphical research for the Devonian sedimentary rocks in the north-northwest of the Song Hien structure’ (project number TNMT.2018.03.05).

Refferences

Bathurst, R.G.C., 1959. The cavernous structure of some Mississippian Stromatactis reefs in Lancashire, England. *Journal of Geology, 67,506-521.*

Bathurst, R.G.C., 1982. Genesis of stromatactis cavities between submarine crusts in Paleozoic carbonate mud buildups. *J. Geol. Soc. London, 139, 165-18.*

Berner, R.A., 1980. Early diagenesis as a theoretical approach. *241 pp., Princeton (Princeton University Press).*

Bosellini, A., Masetti, D., Sarti, M., 1981. A Jurassic 'Tongue of the Ocean infilled with oolitic sands: *The Belluno Trough, Venetian Alps, Italy. - Marine Geol., 44, 59-95, 25 Figs., Amsterdam.*

Bosence, D.W.J., Wood, J.L., Rose, E.P.F., Qing, H., 2000. Low- and high-frequency sealevel changes control peritidal carbonate cycles, facies and dolomitization in the Rock of Gibraltar (Early Jurassic, Iberian Peninsula). J. Geol. Soc. London 157, 61–74.

Coplen, T.B., Kendall, C. and Hopple, J., 1983. Comparison of stable isotope reference samples. *Nature, 302: 236-238*.

Dehler, C.M., Elrick, M., Karlstrom, K.E., Smith, G.A., Crossey, L.J., Timmons, J.M., 2001. Neoproterozoic Chuar Group (~800–742Ma), Grand Canyon: a record of cyclic marine deposition during global cooling and supercontinent rifting. *Sed. Geol. 141–142, 465–499.*

Deprat, J., 1915. Etudes geologiques sur la region septentrionale du Haut Tonkin. *C. R. Acad. Sci. France, 161/25, Paris.*

Deprat, J., 1915. Sur la découverte du Cabrien moyen et supériour au Tonkin, au Kuangsi et dans le Yunnan méridional. C. R. Acad. *Sci. France, T. 161, N. 25, p. 794-796. Paris.*

Deprat, J., 1916. Sur la découverte d' horizons fossilifères nombreux et sur le succession des faunes dans le Cambrien moyen et le Cambrien supéricur du Yunnan méridional. C. R. Acad. *Sci. France, T. 163, p. 761-763. Paris.*

Dickson, J.A.D., 1966. Carbonate identification and genesis as revealed by staining. *J Sediment Petrol 36:491–505.*

Dovjikov, A. E., (ed) et al., 1965. The Geology of the Northern part of Vietnam. *Geological Survey of Vietnam. (in Vietnamese).*

Dunham, R.J., 1962. Classification of carbonate rocks according to depositional textures. In: Ham WE (ed) Classification of carbonate rocks. *AAPG Mem 1:108–121.*

Dunnington, H. V., 1967. Aspects of diagenesis and shape change in stylolitic limestone reservoirs. *Proc.- World Pet. Congr.* 7, 339-352.

Flügel, E., 2004. Microfacies of carbonate rocks - analysis, interpretation and application. *Springer, Berlin Heidelberg New York, 976 pp.*

Folk, R.L., 1959. Practical petrographic classification of limestones. *AAPG Bulletin, 43: 1-38.*

Folk, R.L., 1962. Spectral subdivision of limestone types. In: Ham, W.E. (ed.): Classification of carbonate rocks. *Geol. Soc. Am. Bull., 1, 62-84.*

Gao, G. and Land, L.S., 1991. Geochemistry of Cambrian-Ordovician Arbuckle Limestone, Oklahoma: Implications for diagenetic $\delta^{18}O$ alteration and secular $\delta^{13}C$ and $^{87}Sr/^{86}Sr$ variation: *Geochimica et Cosmochimica Acta, v. 55, p. 2911–2920.*

Goldhammer, R.K., Dunn, P.A., Hardie, L.A., 1990. Depositional cycles, composite sea-level changes, cycle stacking patterns, and the hierarchy of tratigraphic forcing: examples from Alpine Triassic platform carbonates. *Geol. Soc. Am. Bull., 102, 535–562.*

Guo, B., Sanders, J.E. and Friedman, G.M., 1996. Timing and origin of dedolomite in Upper Wappinger Group (Lower Ordovician) strata, southeastern New York. *Carbonates Evaporites, 11, 113–133.*

Halley, R.B. and Scholle, P.A., 1985. Radiaxial fibrous calcite as early-burial, open-system cement: isotopic evidence from Permian to China. *Geol. Soc. Am. Bull., 69, 261, Tulsa.*

Huyen, D.T., (ed) et al., 2007. Phanerozoic stratigraphy in the Northeast part of Vietnam. Center for Information and Archives of Geology, *Geological Survey of Vietnam. (in Vietnamese).*

Hoefs, J., 2009. Stable Isotope Geochemistry. *Springer-Verlag Berlin Heidelberg.*

Keith, M.L., and Weber, J.N., 1964. Carbon and oxygen composition of selected limestones and fossils. *Geochim. Cosmochim. Acta, v.28, pp.1787-1816.*

Kendall, A.C. and Tucker, M.E., 1973. Radiaxial fibrous calcite: a replacement after acicular carbonate. - *Sedimentology, 20, 365-389, Amsterdam.*

Kendall, A.C., 1985. Radiaxial fibrous calcite: a reappraisal. In: Schneidermann, N. and Harris, P.M. (eds.): Carbonate cements. - Soc. Econ. Paleont. *Min. Spec. Publ., 36, 59-77, 14 Figs., Tulsa.*

Kobayashi, T., 1944. On the Cambrian formations in Yunnan and Haut Tonkin and the Trilobites contained. Jap. *J. geol. geogr, 1991/1-4, Tokyo.*

Kolckmann, C.J., 1992. Vergleichende Untersuchungen an jurassischen Kalkoolithen der zentralen Südalpen. - *Profil, 3, 131-225, , 70 Figs., Stuttgart.*

Land, L.S., 1970. Phreatic versus vadose meteoric diagenesis of limestones: evidence from a fossil water table. *Sedimentology, 14, 175-185, 6 Figs., Amsterdam.*

Leonard, J.E., Cameron, B., Pilkey, O.H., and Friedman, G.M., 1981. Evaluation of cold-water carbonates as a possible paleoclimatic indicator. *Sed. Geol., 28, 1-28, 8 Figs., 1 Tab., Amsterdam.*

Longman, M.W., 1980. Carbonate diagenetic textures from nearsurface diagenetic environments. *Geol. Soc. Am. Bull., 64/4, 461-487, 18 Figs., Tulsa.*

Machel, H.G. and Burton, E.A., 1991. Factors governing cathodoluminescence in calcite and dolomite, and their implications for studies of carbonate diagenesis. In: C. Barker and O.C. Kopp (Editors), Luminescence Microscopy and spectroscopy: qualitative and quantitative applications. *Soc. Econ. Paleont. Min., pp. 37-57., Tulsa*

Machel, H.G., 2004. Concepts and models of dolomitization: a critical reappraisal. In: Braithwaite, C.J.R., Rizzi, G., Darke, G. (Eds.), The geometry and petrogenesis of dolomite hydrocarbon reservoirs. *Geol. Soc. London Spec. Publ., 235, pp. 7–63.*

Mansuy, H., 1915 a. Faunes cambriens du Haut Tonkin. *Mém. Serv. Géol. Indoch., vol. IV, fasc. 2, 35 p., Hanoi.*

Mansuy, H., 1915b. Contrubution à l' étude des faunes de l' Ordovicien et du Gothlandien du Tonkin. *Mém. Serv. Géol. Indoch., vol. IV, fasc. 3, 22 p. Hanoi.*

Mansuy, H., 1916. Faunes Cambriens de l' Extrême-Orient méridional. *Mém. Serv. Géol. Indoch., vol. V, fasc. 1, 48p. Hanoi.*

Metcalfe I., 1998. Paleozoic and Mesozoic geological evolution of the SE Asian region, multidisciplinary constraints and implications for biogeography. In: R. Hall & J.D. Holloway (Editors), *Biogeography and Geological Evolution of SE Asia. Backhuys Publishers, Amsterdam, pp. 25-41.*

Metcalfe, I., 2005. Asia: South-East. In: Selley, R.C., Cocks, L.R.M., Plimer, I.R. (Eds.), *Encyclopedia of Geology, vol. 1. Elsevier, Oxford, pp. 169 - 198.*

Meyers, W.J., 1978. Carbonate cements: their regional distribution and interpretation in Mississippean limestones of southwestern New Mexico. - *Sedimentology, 25, 371-400, 18 Figs., Amsterdam.*

Misik, M., 1966. Tentative classification of veinlets in limestones. - *Geol. Sborn. Slov. Akad. Vied, 17,337-344.*

Misik, M., 1998. Peculiar types of thin veins in the Mesozoic carbonates and silicates of the Western Carpathians. *Geologica Carpathica, 49,27 1-29.*

Montañez, I.P., Read, J.F.,1992. Eustatic control on early dolomitization of cyclic peritidal carbonates: evidence from the Early Ordovician Upper Knox Group, Appalachians. *Geol. Soc. Am. Bull., 104, 872–886.*

Ngan, P.K., 2008. The Cambrian system in Vietnam. Published by the Science and Technique *Publishing House, Hanoi, Vietnam. (in Vietnamese).*

Nie S., Rowleyd.B. and Ziegler A.A., 1990. Constraints on the locations of Asian microcontinents in Paleo-Tethys during the Late Paleozoic. In: W.S. Mckerrow & C.R. Scotese (Editors), Palaeozoic palaeogeography and biogeography. *Geol. Soc.Mem., 12: 397-409.*

Rosenbaum, J. and Sheppard, S.M.F., 1986. An Isotopic Study of Siderites, Dolomites and Ankerites at High-Temperatures. *Geochimica et Cosmochimica Acta, 50(6): 1147-1150.*

Saltzman, M.R., Ripperdan, R.L., Brasier, M.D., Lohmann, K.G., Robison, R.A., Chang W.T., Peng. S., Ergaliev, E.K. and Runnegar, B., 2000. A global carbon isotope excursion (SPICE) during the Late Cambrian: relation to trilobite extinctions, organic-matter burial and sea level. Palaeogeography, *Palaeoclimatology, Palaeoecology 162: 211-223.*

Saltzman, M.R., Runnegar, B. and Lohmann, K.C., 1998. Carbon isotope stratigraphy of the Upper Cambrian (Steptoean Stage) sequence of the eastern Gretab basin: record of a global oceanographic event. *GSA Bulletin, 110: 285-297.*

Saurin, E., 1956. Lexique stratigraphique international. *Asia. Indochine. Vol. III, fasc. 6a.*

Shlanger, S. O., 1964. Petrology of limestones of Guam. *Geol. Surv. Prof. Pap. (US.) 403, D1-D52.*

Sial, A.N., Peralta, S., Ferreira, V.P., Toselli, A.J., Aceñolaza, F.G., Parada, M.A., Gaucher, C., Alonso, R.N. and Pimentel, M.M., 2007. Upper Cambrian carbonate sequences of the Argentine Precordillera and the Steptoean C-Isotope positive excursion (SPICE): Gondwana Research 13 (2008) 437–452.

Thanh, T.D. and Khuc, Vu., (Eds.) 2006. Stratigraphic Units of Vietnam. *Published by the Vietnam National University Publishing House, Hanoi, Vietnam.*

Tinh, H.X., (ed) et al., 1976. Geology and mineral resources of Baolac sheet-scale 1:200.000. *Center for Information and Archives of Geology, Geological Survey of Vietnam. (in Vietnamese).*

Tinh, H.X., (ed) et al., 2001. Geology and mineral resources of Baolac sheet-scale 1:200.000. *Center for Information and Archives of Geology, Geological Survey of Vietnam. (in Vietnamese).*

Tucker, M.E., 1995. Techniques in sedimentology. *Blackwell science, Oxford, 394p.*

Tucker, M.E., and Wright, V.P., 1990. Carbonate Sedimentology. *Blackwell Scientific Publications, London. 310p.*

Védrine, S., Strasser, A., and Hug, W., 2007. Oncoid growth and distribution controlled by sea-level fluctuations and climate (Late Oxfordian, Swiss Jura Mountains): *Facies (2007) 53:535–552, (Springer).*

Wright, V.P., 1983. Morphogenesis of oncoids in the Lower Carboniferous Llanelly Formation of South Wales. - In: Peryt, T.M. (ed.): *Coated grains. - 424-434, 7 Figs., Berlin (Springer).*

Wright, V.P., and Smart, P.L., 1994. Paleokarst (dissolution diageneis): Its occurrence and hydrocarbon exploration significance. [In:] K.H. WOLF & G.V. CHILINGARIAN (Eds.): Diagenesis IV. Developments in Sedimentology, 51, *Elsevier, Amsterdam, 489–502.*

Yoo, C.M., Lee, Y.I., 1998. Origin and modification of early dolomites in cyclic shallow platform carbonates, Yeongheung Formation (middle Ordovician), *Korea. Sed. Geol. 118, 141–157.*

Zempolich, W.G., Erba, E., 1999. Sedimentologic and chemostratigraphic recognition of third-order sequences in resedimented carbonate: the Middle Jurassic Vajont Limestone, Venetian Alps, Italy. - In: Opdyke, B.N., Wilkinson, B.H., 1990. Paleolatitude distribution of Phanerozoic marine ooids and cements. Palaeogeogr., *Palaeoclimat., Palaeoecol., 78, 135-148, 9 Figs., Amsterdam.*

.